An improved model for multiple effect distillation

Citation: Mistry, Karan H., Mohamed A. Antar, and John H. Lienhard V. "An Improved Model for Multiple Effect Distillation." Desalination and Water Treatment 51, no. 4–6 (January 2013): 807–821.

As Published: http://dx.doi.org/10.1080/19443994.2012.703383

Publisher: Desalination Publications

Persistent URL: http://hdl.handle.net/1721.1/89068

Version: Author's final manuscript: final author's manuscript post peer review, without publisher's formatting or copy editing

An improved model for multiple effect distillation

Karan H. Mistry[a], Mohamed A. Antar[b], John H. Lienhard V[a,*]

[a]*Department of Mechanical Engineering, Massachusetts Institute of Technology, Cambridge, USA*
[b]*Department of Mechanical Engineering, King Fahd University of Petroleum and Minerals, Dhahran, Saudi Arabia*

Abstract

Increasing global demand for fresh water is driving research and development of advanced desalination technologies. As a result, a detailed model of multiple effect distillation (MED) is developed that is flexible, simple to implement, and suitable for use in optimization of water and power cogeneration systems. The MED system is modeled in a modular method in which each of the subcomponents is modeled individually and then instantiated as necessary in order to piece together the complete plant model. Modular development allows for studying various MED configurations (such as forward feed, parallel feed, *etc.*) with minimal code duplication. Use of equation oriented solvers, such as Engineering Equation Solver (EES) and JACOBIAN, rather than sequential solvers, simplifies the coding complexity dramatically and also reduces the number of required approximations and assumptions. The developed model is compared to four prominent MED forward feed models from literature: El-Sayed and Silver (1980), El-Dessouky et al. (1998) (Detailed), El-Dessouky et al. (2002) (Basic), and Darwish et al. (2006). Through a parametric analysis, it is found that the present model compares very well with the simple model provided by El-Sayed and Silver while providing substantially more detail in regards to the various temperature profiles within the MED system. Further, the model is easier to implement than the detailed El-Dessouky model while relying on fewer assumptions. The increased detail of the model allows for proper sensitivities to key variables related to input, operating, and design conditions necessary for use in a cogeneration or hybrid system optimization process.

Keywords: MED, desalination, performance ratio, specific area, boiling point elevation, cogeneration, model

1. Introduction

As global demand for fresh water increases, the need for development and implementation of a wide variety of desalination technologies continues to grow. Despite the vast improvements to reverse osmosis in recent years, there is still a need for thermal methods of desalination, especially when dealing with harsh feed waters of high temperature, salinity, or contamination. While multistage flash (MSF) is the dominant type of large-scale thermal desalination currently in use, multiple-effect distillation (MED) is thermodynamically superior and is currently receiving considerable attention as a strong competitor to MSF, especially in the Middle East-Arabian Gulf area. The MED process is characterized by lower energy consumption (≈ 2 kWh/m^3) compared to the MSF process (≈ 4 kWh/m^3) since recirculating large quantities of brine is not

*Corresponding author
Email address: lienhard@mit.edu (John H. Lienhard V)

required. Additionally, MED provides higher overall heat transfer coefficients by utilizing primarily latent-heat transfer and avoiding the lower specific heat transfer surface areas associated with sensible heat transfer found in MSF [1]. The ability to operate at low temperature and use low grade heat from power station turbines as the primary heat source for MED yield very low specific energy costs for seawater desalination and allows the use of lower grade materials for heat transfer tubes (*e.g.*, aluminum alloys) and the evaporator body (*e.g.*, carbon steel epoxy coated shells) [2]. As a result, MED systems are established in many locations within the Kingdom of Saudi Arabia with capacities ranging from 1,500–800,000 m^3/day [3].

However, the high energy consumption associated with desalination processes such as MED, especially as compared to the least work of separation [4], suggests that further research on these and other technologies is needed in order to lower the cost and increase the availability of potable water. One way to accomplish this is to combine thermal desalination systems, such as MED, with electricity production plants in a combined water-power co-generation scheme. Co-generation has the advantage of being able to produce both water and power at lower costs and increased flexibility than if they were produced independently. In this paper, a new MED model is developed that is well-suited for studying and optimizing in a co-generation plant model. The new model is also compared to four MED models from literature and the advantages and limitations of each are discussed.

While there are numerous MED models in the literature, the models by El-Dessouky et al. [5], El-Dessouky and Ettouney [6], Darwish et al. [7] are among the most cited. Additionally, the model by El-Sayed and Silver [8] is very simple, yet based on clear thermodynamic principles. While these models have utility, they do not provide adequate sensitivity to key parameters necessary for a complete co-generation system optimization. Therefore, a new model that relies on fewer assumptions and is solved using a simultaneous equation solver, rather than an iterative sequential solver, is developed.

2. Overview of multiple effect distillation and review of existing models

Accurate system modeling is essential for developing understanding and for exploring possibilities for improvement. As such, numerous MED models have been developed. El-Sayed and Silver [8] developed one of the earliest forward feed MED models and were able to calculate performance ratio and heat transfer areas through several simplifying thermodynamic assumptions. El-Dessouky et al. [5], El-Dessouky and Ettouney [9], El-Dessouky et al. [10] analyzed different MED configurations including the parallel flow, the parallel/cross flow, and systems combined with a thermal vapor compressor (TVC) or mechanical vapor compressor (MVC). The heat transfer equations used in the model assume that the area calculated is the sum of the area of brine heating and the area for evaporation. They found that the thermal performance ratio of the TVC and specific power consumption of the MVC decrease at higher heating steam temperatures. In addition, increasing heating steam temperature reduces the specific heat transfer area. The conversion ratio is found to depend on the brine flow configuration and to be independent of the vapor compression mode. El-Dessouky and Ettouney [6] also developed a simplified model. Darwish et al. [7], Darwish and Abdulrahim [11] also developed a simple MED model and analyzed various configurations and discussed the trade off between performance ratio and required heat transfer area.

El-Allawy [12] examined how the gained output ratio (GOR) of an MED (with and without TVC) system varied with top brine temperature (TBT) and number of effects. Results revealed that increase of number of effects from 3 to 6 result in the increase of the GOR by nearly two-fold. Aly and El-Figi [13] developed a steady state mathematical model to study the performance of forward feed MED process and found that the performance ratio is significantly dependent on the number of rather than the top brine temperature. Al-Sahali and Ettouney [14] developed simple simulation model for MED-TVC based on a sequential solution method,

rather than iterative procedure while assuming constant temperature drop, specific heat, and heat transfer coefficients. Ameri et al. [15] studied the effect of design parameters on MED system specifications and found that optimum performance depends on an optimum number of effects which itself depends on sea water salinity, feed water temperature, and effect temperature differences. Kamali and Mohebinia [16] developed a simulation program to improve the performance of an existing MED unit of 7 effects and nominal production of 1,800 m^3/day. They found that the unit production increased by 15% with the same top brine temperature of 70 °C by increasing the area of condenser tubes by 32%.

Kamali et al. [17] optimized the performance of actual MED producing 1500 ton/day whereas Darwish and Alsairafi [3] compared MSF with MED using a simple simulation model assuming equal vapor generated by boiling in all effects, equal boiling temperature difference between effects, and equal specific heat. They reported that MED is favored on MSF by less shell volume of order half of that of MSF, lower pumping energy, less treatment of feed, and lower temperature losses. For a constant flux of 12.6 kW/m^2, Minnich et al. [18] reported that the optimum GOR and TBT were found to be 14 and 110 °C, respectively. They added that limiting TBT of MED to 60 °C prevents the system from utilizing higher heat transfer coefficients and constant temperature difference that drives the heat transfer.

Second Law analysis for MED was conducted by [19–21] where the major subsystems for exergy destruction were the TVC and effects which accounted more than 70% of the total amount. Hamed [22], Hamed et al. [23] investigated the thermal performance of the MED desalination system at different variables including number of effects, TBT, and inlet seawater. He concluded that the performance ratio increased with increasing number of effects while TBT and inlet seawater a slight affect on plant performance. Greogorzewski and Genthner [24] reported an analytical study restricted to different configurations of MED systems without TVC.

Four models from literature are considered in more detail.

2.1. El-Sayed and Silver

El-Sayed and Silver [8] developed a simple model for a forward feed (FF) MED system with flash evaporation (Fig. 1). All fluid properties are assumed constant [mean latent heat ($\bar{h}_{fg}$), specific heat (c), and boiling point elevation (BPE)]. The fluids are assumed to be an ideal solution and the pressure drop due to friction is modeled based on a mean saturation temperature drop augmented by the effect of BPE. Based on these assumptions, El-Sayed and Silver explicitly solve for the performance ratio of the system:

$$\mathrm{PR} = \frac{h_{fg,S}}{\dfrac{\bar{h}_{fg}}{n} + \dfrac{\dot{m}_F}{\dot{m}_D} c\,(\mathrm{TTD}_{fh} + \epsilon) + \dfrac{n-1}{2n} c \Delta T_e} \tag{1}$$

where $h_{fg,S}$ is the enthalpy of vaporization of steam, n is the number of effects, $\dot{m}_F$ and $\dot{m}_D$ are the mass flow rates of feed and distillate, TTD_{fh} is the terminal temperature difference in the feed heaters, ϵ is the sum of BPE and temperature change due to pressure loss, and ΔT_e is a temperature difference between two effects. Additional equations are provided for calculating the required heat transfer surface area as a function of a known or assumed overall heat transfer coefficient.

Despite its simplicity, Eq. (1) is derived using strong thermodynamic arguments and is useful for quickly approximating the performance ratio and required transfer areas for an MED-FF system under known operating conditions. However, it cannot be used to find detailed information regarding various specific streams or to understand system sensitivities to various parameters.

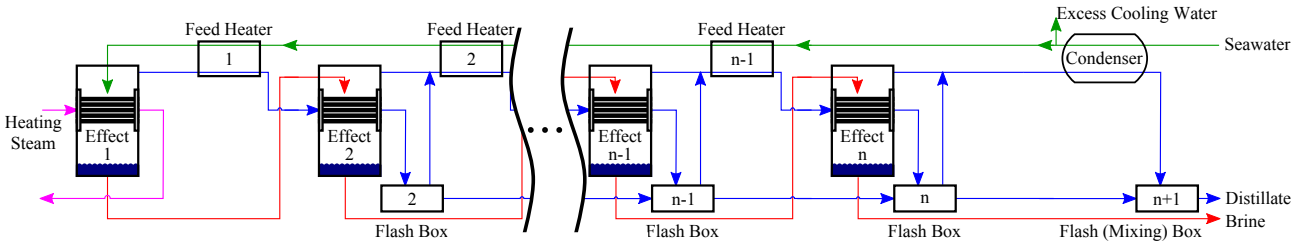

Figure 1: In a forward feed MED system, the feed water is preheated by condensing distillate vapor from the effects and flash boxes prior to being injected into the first effect to reduce the amount of required heating steam. Water vapor is removed from the feed stream in each effect until the brine is eventually discharged from the final effect.

2.2. Darwish et al.

Darwish et al. [7] developed a simple model for MED-FF with flash evaporation while assuming that: equal vapor is generated by boiling in each effect other than the first ($D_b = \beta \dot{m}_D$), equal boiling temperature difference between effects (ΔT_e), equal temperature increase of the feed in feed heaters (ΔT_{fh}) and $\Delta T_e = \Delta T_{fh}$, equal specific heat for the brine and feed, equal latent heat (h_{fg}) and BPE. Using these assumptions, Darwish et al. simplified the MED-FF system and approximated the performance ratio for the system:

$$\mathrm{PR} = \frac{\dot{m}_D}{\dot{m}_S} = \frac{n}{1 + n\dfrac{\dot{m}_F c(\mathrm{TTD}_{fh})}{\dot{m}_D \bar{h}_{fg}}} \tag{2}$$

where $\dot{m}_F$, $\dot{m}_D$, and $\dot{m}_S$ are the mass flow rates of feed, distillate, and steam respectively, c is the specific heat, h_{fg} is the latent heat, and TTD_{fh} is the temperature difference between the first effect and the feed at the exit of the last feed heater.

2.3. El-Dessouky and Ettouney Basic Model

El-Dessouky and Ettouney [6] presented a simplified MED mathematical model where the data generated are related only to brine and distillate flow rates, brine concentration, temperature and heat transfer area. Heat and mass balances for flash boxes and pre-heaters are excluded and it is assumed that the feed enters the first effect at the first effect's saturation temperature (*i.e.*, steam is used only to evaporate distillate in the first effect, not for heating the feed). This model relies on the following assumptions: specific heat is constant at an average temperature, thermodynamic losses are constant across all effects, no vapor flashes in the effects, produced vapor is salt-free, equal thermal loads in all effects, driving temperature difference in the effects is equal to the difference in condensation and evaporation temperatures, and negligible energy losses to the environment. Convergence is achieved while equating the heat transfer area in all effects. Although this greatly simplified model does not address fully practical plants, it provides basic understanding to the process involved in MED desalination.

2.4. El-Dessouky and Ettouney Detailed Model

El-Dessouky et al. [5] also presented a detailed MED model that takes into account the pre-heaters and flashing boxes in an MED-FF system (Fig. 1). The model assumes constant heat transfer areas for both the evaporators and feed pre-heaters in all effects. In addition, the model considers the impact of the vapor leak in the venting system, the variation in thermodynamic losses from one effect to another, the dependence of the physical properties of water on

salinity and temperature, and the influence of non-condensable gases on the heat transfer coefficients in the evaporators and the feed pre-heaters. Several correlations are used in this model, particularly to determine the heat transfer coefficients and pressure losses. Two correlations are developed to relate the heat transfer coefficients in the pre-heater and the evaporator to the boiling temperature. Design correlations are also developed to describe variations in the plant thermal performance, the specific heat transfer area, and the specific flow rate of cooling water in terms of the top brine temperature and the number of effects. Calculations showed that the heat transfer coefficient in the evaporators are greater than those in the pre-heaters and that the effect of TBT on the specific heat transfer area is more pronounced at high number of effects.

3. An improved MED model

A thermal model of an MED system is presented that provides a more accurate description of the MED process through relying on fewer assumptions and simplifications. Unlike most of the models in the literature, the present model is solved using a simultaneous equation solver.

3.1. Approximations

Several standard engineering approximations are made in this analysis:

- Steady state operation.
- Distillate is pure water (*i.e.*, salinity of product water is 0 g/kg).
- Exchanger area in the effects is just large enough to condense vapor to saturated liquid (i.e., $x = 0$) at the previous effect's pressure.
- Seawater is an incompressible liquid and the properties are only a function of temperature and salinity.
- Energy losses to the environment are negligible.
- Non-equilibrium allowance (NEA) is negligible [6].
- Brine (liquid) and distillate (vapor) streams leave each effect at that effect's temperature. Distillate vapor is slightly superheated.
- The overall heat transfer coefficient is averaged over the length of an exchanger.
- The overall heat transfer coefficient in each effect, feed heater, and condenser is a function of temperature only [6].

3.2. Software and solution methodology

While most of the existing models in literature are developed to be solved using an iterative procedure in a sequential numerical package such as MATLAB [25], the present model was developed using a simultaneous equation solver. A fundamental advantage of using an equation solver is that the programmer does not need to develop algorithms for reaching solution convergence. Instead, the governing equations are inputted much as one would write them on paper. The solver then identifies and groups the equations that must be solved and solves for the system iteratively. During the development process, the model was implemented using two different software packages: Engineering Equation Solver (EES) [26] and JACOBIAN [27].

3.3. Physical properties

Accurate physical properties for seawater and water vapor are used. Seawater, approximated as an incompressible fluid, properties are evaluated as a function of temperature and salinity [28]. All liquid water states are modeled using this seawater property package: pure water is modeled as seawater with 0 salinity. Vapor phase water properties are calculated using the fundamental equations of state provided by IAPWS. EES uses the IAPWS 1995 Formulation [29] while the IAPWS 1997 Industrial Formulation [30] was implemented for use in JACOBIAN. Differences between the two formulations are negligible.

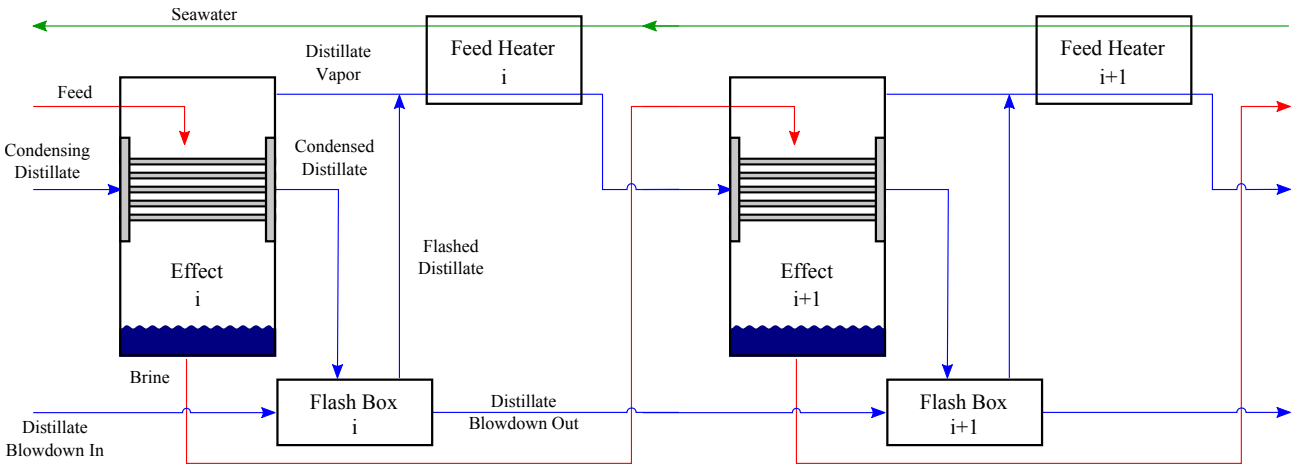

Figure 2: Detailed view of the stream connections between each of the components in an MED system.

3.4. Component models

Since MED systems are composed of multiple identical stages, there are several components that are utilized numerous times. In order to simplify the model, each component is modeled individually. The overall system model is then created by instantiating each component the necessary number of times and adding additional equations to connect the various components in the appropriate manner. Component models for the effects, feed heaters, flash boxes, and condenser are presented below. A schematic diagram showing a typical configuration of a forward feed MED system is illustrated in Fig. 1. A detailed schematic diagram showing the fluid stream connections between components is shown in Fig. 2.

3.4.1. Effects

The effect is the primary component in an MED system. Feed water (F) is sprayed into the effect over a series of tubes. Distillate vapor (D_c) from the previous effect condenses in these tubes. Typically, the effect is maintained at a pressure slightly below the saturation pressure of the feed water which causes a small fraction of the feed to flash evaporate (D_f). As the D_c, it releases the heat of vaporization which is transfered to the feed resulting in the creation of more vapor (D_b). The vapor produced through both flashing and boiling (D) as well as the brine (B) are then extracted from the effect (Fig. 2). Note: each of the variables should be indexed with an i to indicate that these are array variables; however, for clarity, the index is neglected. A control volume showing the relevant variables that characterize the effect's inlet and outlet streams is presented in Fig. 3.

Water balance: The feed stream is split into a distillate (vapor) stream and a brine stream. Prior to the evaporation from boiling (internal to the effect), the feed stream can be divided into a brine stream within the effect (B_e) and the distillate formed from flashing. The total distillate produced is the sum of that formed from flashing and boiling.

$$F = B + D \tag{3}$$

$$F = B_e + D_f \tag{4}$$

$$D = D_b + D_f \tag{5}$$

Salt balance: Salinity of the brine stream within the effect (X_{B_e}) and the brine stream leaving the effect (X_B) is found found through a salt balance in which it is assumed that both

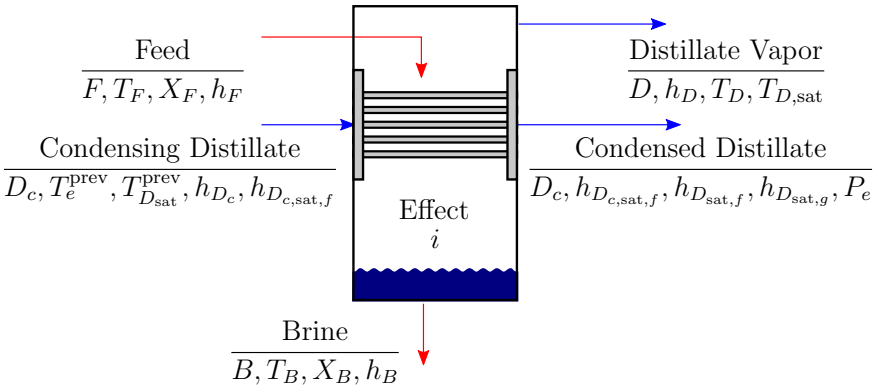

Figure 3: Variables associated with the inlet and outlet streams of the i^{th} effect.

the distillate formed through flashing and boiling is pure (*i.e.*, $X_{D_f} = X_{D_b} = 0$ g/kg).

$$FX_F = BX_B \tag{6}$$
$$FX_F = B_eX_{B_e} \tag{7}$$

Energy balance: The change in enthalpy associated with the condensation of the distillate from the previous effect is used to separate the feed stream into new brine and distillate streams.

$$D_c\Delta h_{D_c} = Dh_D + Bh_B - Fh_F \tag{8}$$

The value of Δh_{D_c} is discussed below as it is different for the first and the second through n^{th} effects.

Distillate saturation temperature: Salinity causes the boiling point to be elevated. Distillate formed in the effect is superheated by an amount equal to the BPE. The distillate will condense at the saturation temperature in the following feed heater and effect.

$$T_{D_{\text{sat}}} = T_D - \text{BPE}_D \tag{9}$$

Heat transfer area: The condensate tube surface area must be large enough to ensure that the distillate vapor from the previous effect condenses completely while heating and evaporating the feed. Since there is phase change on both sides of the tubes, the rate of heat transfer is best modeled by Newton's Law of Cooling, where the heat transfered is equal to the change in enthalpy associated with the condensation of distillate [*cf.*, Eq. (8)].

$$D_c\Delta h_{D_c} = A_eU_e(T_{D_{\text{sat}}}^{\text{prev}} - T_e) \tag{10}$$

The temperature at which the distillate from the previous effect condenses is equal to the saturation temperature of the previous effect, $T_c = T_{D_{\text{sat}}}^{\text{prev}}$. The overall heat transfer coefficient in Eq. (10) is calculated using a correlation from El-Dessouky and Ettouney [6]:

$$\begin{aligned} U_e = 10^{-3}\times \big[&1939.1 + 1.40562(T_{D_{\text{sat}}}^{\text{prev}} - 273.15) \\ &-0.0207525(T_{D_{\text{sat}}}^{\text{prev}} - 273.15)^2 \\ &+0.0023186(T_{D_{\text{sat}}}^{\text{prev}} - 273.15)^3\big] \end{aligned} \tag{11}$$

where U_e is in kW/m^2-K and $T_{D_{\text{sat}}}^{\text{prev}}$ is in K. The correlations provided by El-Dessouky et al. serve as a good approximation for the overall heat transfer coefficient values. If a model is being developed for an actual physical plant, more accurate U values can be obtained by analyzing

the heat transfer processes occurring in the particular geometry.

Fluid properties: The temperature of the brine (T_B) and distillate vapor (T_D) is equal to the effect temperature (T_e). The boiling point elevation (BPE_D), effect pressure (P_e), enthalpy of brine after flashing (h_{B_e}), enthalpy of brine (h_B), enthalpy of distillate [from boiling (h_{D_b}), from flashing (h_{D_f}), and total (h_D)], and enthalpies of saturated water ($h_{D_{\mathrm{sat},f}}$) and vapor ($h_{D_{\mathrm{sat},g}}$) are all evaluated as a function of temperature, pressure, and salinity as discussed in Section 3.3.

Some useful temperature differences include the terminal temperature difference in the effect (TTD_e), which is the temperature of condensation minus the effect temperature, and the temperature difference between effects (ΔT_e).

$$\mathrm{TTD}_e = T_c - T_e \tag{12}$$

$$\Delta T_e = T_e^{\mathrm{prev}} - T_e \tag{13}$$

First effect

While the hardware for all effects is identical, there are two slight differences between the first effect and the remaining ones. First, feed enters the first effect below the saturation temperature (subcooled) where as in all subsequent effects, feed enters slightly above the saturation temperature (superheated). Second, steam is used to heat the feed in the first effect while the vapor produced in the previous effect is used to heat the feed in all the subsequent effects. Flashing does not occur in the first effect because the feed stream is subcooled when it enters the first effect.

$$D_f = 0 \tag{14}$$

Steam input to the first effect can be accounted for by modifying the effect's energy balance [Eq. (8)] to be based on the steam flow rate ($\dot{m}_S$) and latent heat of vaporization (λ_S):

$$D_c \Delta h_{D_c} \rightarrow \dot{m}_S h_{fg,S} \tag{15}$$

Second through n^{th} effect

In all subsequent effects, a portion of the feed stream flashes. An additional energy balance equation [complement to Eq. (4)] is needed to fully define the effect.

$$F h_F = B_e h_{B_e} + D_f h_{D_f} \tag{16}$$

The enthalpy change of the distillate during condensation may not be equal to the latent heat of vaporization since the distillate from the previous effect may enter the effect as superheated vapor, saturated vapor, or two-phase. It is assumed that complete condensation occurs. Therefore, the change in enthalpy in Eq. (8) is defined as:

$$\Delta h_{D_c} = h_{D_c} - h_{D_{c,\mathrm{sat},f}} \tag{17}$$

where h_{D_c} is the enthalpy of the distillate at the entrance to the effect's condensing tube.

3.4.2. Flash box

The condensed distillate from each effect is collected with all of the condensed distillate from the previous effects. As the distillate is collected in each stage, the distillate pressure is decreased in the flash boxes to correspond with the pressure of the current effect. Part of the distillate blowdown from the previous effect ($D_{\mathrm{bd}}^{\mathrm{in}}$) and the distillate used for condensing in the current effect (D_c) is flashed during the depressurization. The newly produced vapor, D_{fb}, is sent to the feed heater and the remaining liquid distillate, D_{bd} is sent to the next flash box (Fig. 2). Both D_{fb} and D_{bd} are at p_e. Note: each of the variables should be indexed with an i to indicate that these are array variables; however, for clarity, the index is neglected. A control

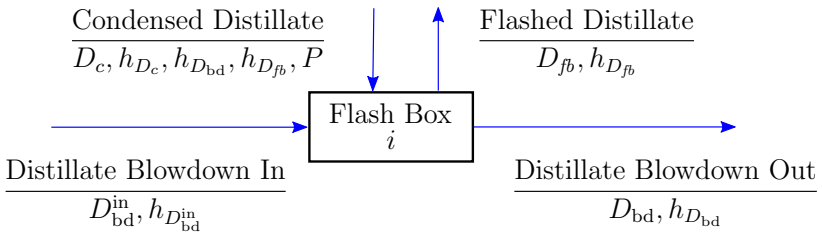

Figure 4: Variables associated with the inlet and outlet streams of the i^{th} flash box.

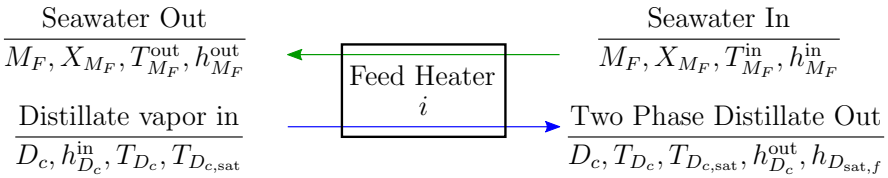

Figure 5: Variables associated with the inlet and outlet streams of the feed heater.

volume showing the relevant variables that characterize the flash box's inlet and outlet streams is presented in Fig. 4.

The mixing and flashing process are governed by mass conservation and the First Law of Thermodynamics:

$$D_{\text{bd}} + D_{fb} = D_{\text{bd}}^{\text{in}} + D_c \tag{18}$$

$$D_{\text{bd}} h_{D_{\text{bd}}} + D_{fb} h_{D_{fb}} = D_{\text{bd}}^{\text{in}} h_{D_{\text{bd}}^{\text{in}}} + D_c h_{D_c} \tag{19}$$

Distillate blowdown temperature can be evaluated as a function of the blowdown enthalpy and pressure.

3.4.3. Mixing box

No flashing occurs in the flash box when all inlet and outlet streams are at the same pressure and the flash box acts as a mixing vessel. The flash box equations can be reduced with the following two equations.

$$D_{fb} = 0 \tag{20}$$

$$h_{D_{fb}} = \text{undefined} \tag{21}$$

The mixing box is only used to recombine the condensed distillate from the condenser with that from the final flash box (Fig. 1).

3.4.4. Feed heater

Feed heaters are used to recover energy and reduce the amount of steam required for heating the feed in the first effect. In each feed heater, some of the distillate vapor from the effect and the flash box condenses and the heat released is used to heat the seawater (Fig. 2). Note: each of the variables should be indexed with an i to indicate that these are array variables; however, for clarity, the index is neglected. A control volume showing the relevant variables that characterize the feed heater's inlet and outlet streams is presented in Fig. 5.

An energy balance and the log mean temperature difference (LMTD) method are used to

calculate the required heat transfer area.

$$D_c \left(h_{D_c}^{\text{in}} - h_{D_c}^{\text{out}}\right) = \dot{m}_F \left(h_{\dot{m}_F}^{\text{out}} - h_{\dot{m}_F}^{\text{in}}\right) \tag{22}$$

$$D_c \left(h_{D_c}^{\text{in}} - h_{D_c}^{\text{out}}\right) = A_{fh} U_{fh} \frac{T_{\dot{m}_F}^{\text{in}} - T_{\dot{m}_F}^{\text{out}}}{\ln \dfrac{T_{D_{c,\text{sat}}} - T_{\dot{m}_F}^{\text{out}}}{T_{D_{c,\text{sat}}} - T_{\dot{m}_F}^{\text{in}}}} \tag{23}$$

The overall heat transfer coefficient in Eq. (23) is calculated using a correlation from El-Dessouky and Ettouney [6]:

$$\begin{aligned} U_{fh} = 10^{-3} \times \big[&1617.5 + 0.1537(T_{D_{c,\text{sat}}} - 273.15) \\ &+0.1825(T_{D_{c,\text{sat}}} - 273.15)^2 \\ &-0.00008026(T_{D_{c,\text{sat}}} - 273.15)^3\big] \end{aligned} \tag{24}$$

where U_{fh} is in kW/m^2-K and $T_{D_{c,\text{sat}}}$ is in K. While the log mean temperature difference method is used here, the ε-NTU method yields equivalent results since the feed heaters are essentially single stream heat exchangers.

The minimum temperature difference in the feed heater occurs at the outlet of the seawater.

$$T_{D_c} - T_{\dot{m}_F}^{\text{out}} = \text{TTD}_{fh} \tag{25}$$

Enthalpy of the seawater leaving the feed heater is calculated based on the outlet temperature and salinity.

3.4.5. Condenser

Distillate from the final effect and flash box is condensed in a condenser, which is essentially a large feed heater. Typically, excess seawater is required in order to meet the required cooling load. Excess seawater is used for cooling purposes alone and is returned to the source after being exhausted from the condenser while the required feed is sent to the first feed heater. Energy balance and heat transfer area calculations for the condenser are similar to those for the feed heaters:

$$D_c \Delta h_{D_c} = \dot{m}_{\text{cond}} \left(h_{sw}^{\text{out}} - h_{sw}^{\text{in}}\right) \tag{26}$$

$$\dot{m}_{\text{cond}} \left(h_{sw}^{\text{out}} - h_{sw}^{\text{in}}\right) = A_c U_c \frac{T_{sw}^{\text{out}} - T_{sw}^{\text{in}}}{\ln \left(\dfrac{T_D - T_{sw}^{\text{in}}}{T_D - T_{sw}^{\text{out}}}\right)} \tag{27}$$

The overall heat transfer coefficient in Eq. (27) is calculated using a correlation from El-Dessouky and Ettouney [6]:

$$\begin{aligned} U_c = 10^{-3} \times [&1617.5 + 0.1537(T_D - 273.15) \\ &+0.1825(T_D - 273.15)^2 \\ &-0.00008026(T_D - 273.15)^3] \end{aligned} \tag{28}$$

where U_c is in kW/m^2-K and T_D is in K. While the log mean temperature difference method is used here, the ε-NTU method yields equivalent results since the condenser is essentially a single stream heat exchanger.

Inlet and outlet seawater enthalpies are calculated as a function of the respective temperatures and the feed salinity.

3.5. MED-FF with flash box regeneration system model

Numerous MED system configurations can be created by piecing together the component models presented in Section 3.4. Equations for connecting the relevant components to form the typical MED-FF configuration shown in Fig. 1 are outlined below. Note that all of the equations are simply matching (or combining) variables from one component to another.

Typical MED systems utilize flash boxes and feed heaters in order to collect the distillate and preheat the seawater prior to injection into the first effect (Fig. 1) [5–8]. An advantage of this configuration is that high energy recovery can be achieved while using relatively simple components.

3.5.1. Match streams between components

The distillate (D_c) output (in 2 phase state) from the i^{th} feed heater effect is used as the condensing distillate input in the i^{th}+1 effect. The distillate flow rate, temperature, saturation temperature, present enthalpy, and saturated liquid enthalpy must be passed to the i^{th}+1 effect.

For $i \in \{1, \ldots, n-1\}$:

$$\frac{\text{Feed heater, } i}{D_c, T_{D_c}, T_{D_{c,\text{sat}}}, h_{D_c}^{\text{out}}, h_{D_{\text{sat},f}}} \quad \longrightarrow \quad \frac{\text{Effect, } i+1}{D_c, T_e^{\text{prev}}, T_{D_{\text{sat}}}^{\text{prev}}, h_{D_c}, h_{D_{c,\text{sat},f}}}$$

Brine from the i^{th} effect is used as feed for the i^{th}+1 effect. Brine flow rate, temperature, salinity, and enthalpy is passed to the i^{th}+1 effect.

For $i \in \{1, \ldots, n-1\}$:

$$\frac{\text{Effect, } i}{B, T_B, X_B, h_B} \quad \longrightarrow \quad \frac{\text{Effect, } i+1}{F, T_F, X_F, h_F}$$

Distillate boxes

As the distillate condenses in each effect, it is mixed with all of the distillate from the previous effects. The pressure of the distillate is decreased to correspond with the pressure in the effects. As a result, a portion of the distillate flashes and the vapor is then sent to the feed heaters. There is no flash box for the first effect (Fig. 1). For programming convenience, the flash box index begins with 2, rather than 1.

Distillate from the first effect does not mix with distillate from a (non-existent) previous effect. In order to reuse the flash box code, the blowdown input to the first flash box ($D_{\text{bd}}^{\text{in}}, h_{D_{\text{bd}}}^{\text{in}}$) is set to zero.

$$\frac{\text{Effect, } 2}{D_c, h_{D_{c,\text{sat},f}}, h_{D_{\text{sat},f}}, h_{D_{\text{sat},g}}, P_e} \quad \longrightarrow \quad \frac{\text{Flash box, } 2}{D_c, h_{D_c}, h_{D_{\text{bd}}}, h_{D_{fb}}, P}$$

For flash boxes 3–n, the inputs are blowdown distillate from the previous distillate box and the newly condensed distillate from the current effect. The output is saturated vapor (to feed heater) and liquid (blowdown to next box).

For $i \in \{2, \ldots, n-1\}$:

$$\frac{\text{flash box, } i}{D_{\text{bd}}, h_{D_{\text{bd}}}} \quad \longrightarrow \quad \frac{\text{flash box, } i+1}{D_{\text{bd}}^{\text{in}}, h_{D_{\text{bd}}}^{\text{in}}}$$

For $i \in \{3, \ldots, n\}$:

$$\frac{\text{Effect, } i}{D_c, h_{D_{c,\text{sat},f}}, h_{D_{\text{sat},f}}, h_{D_{\text{sat},g}}, P_e} \quad \longrightarrow \quad \frac{\text{flash box, } i}{D_c, h_{D_c}, h_{D_{\text{bd}}}, h_{D_{fb}}, P}$$

The final flash box is a mixing vessel to combine the distillate blowdown from the n^{th} distillate box and the distillate that was condensed in the condenser.

$$\frac{\text{flash box, } n}{D_{\text{bd}}, h_{D_{\text{bd}}}} \longrightarrow \frac{\text{flash box, } n+1}{D_{\text{bd}}^{\text{in}}, h_{D_{\text{bd}}^{\text{in}}}}$$

$$\frac{\text{Effect, } n}{h_{D_{\text{sat},f}}} \longrightarrow \frac{\text{flash box, } n+1}{h_{D_c}}$$

Unlike the previous flash boxes, the newly condensed distillate comes from the condenser.

$$\frac{\text{Condenser}}{D_c} \longrightarrow \frac{\text{flash box, } n+1}{D_c}$$

Feed heaters

Seawater is heated in the i^{th} feed heater by distillate vapor from both the i^{th} effect and the i^{th} flash box. The enthalpy of the mixture of distillate vapors is the mass weighted average.

For $i \in \{1, \ldots, n-1\}$:

$$D_c\big|_{\text{Feed heater},i} = D\big|_{\text{Effect},i} + D_{fb}\big|_{\text{Flash box},i}$$
$$(D_c h_{D_c}^{\text{in}})\big|_{\text{Feed heater},i} = (Dh_D)\big|_{\text{Effect},i} + (D_{fb}h_{D,fb})\big|_{\text{Flash box},i}$$

$$\frac{\text{Feed heater, } i}{T_{D_c}, T_{D_{c,\text{sat}}}} \longrightarrow \frac{\text{Effect, } i}{T_D, T_{D_{\text{sat}}}}$$

For feed heaters 1 through $n-2$, the output of one feed heater is the input to the next. Note that the seawater is flowing from higher numbered feed heater to lower numbered feed heater.

For $i \in \{1, \ldots, n-2\}$:

$$\frac{\text{Feed heater, } i+1}{\dot{m}_F, X_{\dot{m}_F}, T_{\dot{m}_F}^{\text{out}}, h_{\dot{m}_F}^{\text{out}}} \longrightarrow \frac{\text{Feed heater, } i}{\dot{m}_F, X_{\dot{m}_F}, T_{\dot{m}_F}^{\text{in}}, h_{\dot{m}_F}^{\text{in}}}$$

The initial feed heater, $n-1$, is fed seawater from the output of the condenser:

$$\frac{\text{Condenser}}{X_{sw}, T_{sw}^{\text{out}}, h_{sw}^{\text{out}}} \longrightarrow \frac{\text{Feed heater, } n-1}{X_{\dot{m}_F}, T_{\dot{m}_F}^{\text{in}}, h_{\dot{m}_F}^{\text{in}}}$$

A condenser is used to condense the distillate vapor from the n^{th} effect and n^{th} flash box. The enthalpy of the mixture of distillate vapors is the mass weighted average.

$$D_c\big|_{\text{Condenser}} = D\big|_{\text{Effect},n} + D_{fb}\big|_{\text{Flash box},n}$$
$$(D_c h_{D_c}^{\text{in}})\big|_{\text{Condenser}} = (Dh_D)\big|_{\text{Effect},n} + (D_{fb}h_{D,fb})\big|_{\text{Flash box},n}$$

The change in enthalpy associated with condensation of the vapor in the condenser is

$$\Delta h_{D_c}|_{\text{Condenser}} = h_{D_c}^{\text{in}}|_{\text{Condenser}} - h_{D_{\text{sat},f}}|_{\text{Effect},n}$$

$$\frac{\text{Effect, } n}{T_D} \longrightarrow \frac{\text{Condenser}}{T_D}$$

The seawater feed into the first effect is the warm seawater output from the last feed heater.

$$\frac{\text{Feed heater, 1}}{T^{\text{out}}_{\dot{m}_F}, X_{\dot{m}_F}, h^{\text{out}}_{\dot{m}_F}} \quad \longrightarrow \quad \frac{\text{Effect, 1}}{T_F, X_F, h_F}$$

The flow rate of feed into the first effect is $F(1) = \dot{m}_F$. Since a portion of the seawater through the condenser is returned to the source, $\dot{m}_{\text{cond}} \geq \dot{m}_F$.

There are two options for constraining the size of the effects. In order to reduce the cost of the system, MED plants are typically built with effects of equal area. If, however, it is desired to have a constant temperature drop across each effect, the temperature difference between effects can be specified instead.

$$A_e(i) = A_e(1) \qquad i \in \{2, \ldots, n\} \tag{29}$$

or

$$\Delta T_e(i) = \Delta T_e(1) \qquad i \in \{2, \ldots, n\} \tag{30}$$

Similarly, there are two options for constraining the size of the feed heaters. To reduce the cost of the system, all feed heaters should have the same area. However, it may be desired to have the same TTD in each feed heater.

$$A_{fh}(i) = A_{fh}(1) \qquad i \in \{2, \ldots, n-1\} \tag{31}$$

or

$$\text{TTD}_{fh}(i) = \text{TTD}_{fh}(1) \qquad i \in \{2, \ldots, n-1\} \tag{32}$$

The amount of water produced is equal to the sum of the distillate produced in each effect. The mass flow rate of steam required is equal to the amount of vapor that must condense in the first effect. The amount of seawater feed required is equal to the feed flow rate in the first effect. The amount of excess cooling is the difference between $\dot{m}_{\text{cond}}$ and $\dot{m}_F$. The final brine flow rate is the difference between the feed and distillate flow rate.

$$\dot{m}_D = \sum_{i=1}^{n} D(i) \tag{33}$$

$$\dot{m}_S = D_c(1) \tag{34}$$

$$\dot{m}_F = F(1) \tag{35}$$

$$\dot{m}_B = B(n) \tag{36}$$

3.5.2. Required inputs

Feed, steam, operating, and design conditions are required in order to fully specify the flash box based MED-FF model. Number of effects must be specified. Seawater is fully characterized by temperature and salinity (T^{in}_{sw}, X^{in}_{sw}). Steam is fully characterized by its saturation temperature since it is assumed that it enters the first effect as saturated vapor and leaves the first effect as saturated liquid. The following variables are set based on the steam temperature:

$$T^{\text{prev}}_e = T_S \tag{37}$$

$$T^{\text{prev}}_{D_{\text{sat}}} = T_S \tag{38}$$

$$h_{D_c} = h_g(T_S) \tag{39}$$

$$h_{D_{c,\text{sat},f}} = h_f(T_S) \tag{40}$$

For on-design analysis, the following system characteristics must be specified:

- temperature of the last effect, or a terminal temperature difference between the last effect

and the condenser

- mass flow rate of the distillate, feed, or brine
- maximum allowable salinity (or recovery ratio)
- temperature rise in the condenser
- minimum TTD in the feed heaters

Off-design analysis can be performed by inputting area of the effects, feed heaters, and condenser rather than maximum salinity, temperature rise, and TTDs.

3.5.3. Performance parameters

Once the above equations have been solved, the productivity ratio (PR), recovery ratio (RR), and specific area (SA) are all calculated.

$$\mathrm{PR} = \frac{\dot{m}_D}{\dot{m}_S} \tag{41}$$

$$\mathrm{RR} = \frac{\dot{m}_D}{\dot{m}_F} \tag{42}$$

$$\mathrm{SA} = \frac{\sum A_e + \sum A_{fh} + A_c}{\dot{m}_D} \tag{43}$$

3.5.4. Pressure drops and pumping work

In general, the pressure drop in a condenser is the sum of the pressure drops due to various inlet and exit losses, static head, momentum change, and two-phase friction loss. When considering condensers operating at vacuum conditions, the momentum change results in a pressure regain and the magnitude of the regain may be of the same order of magnitude (might even exceed) as the pressure losses [31]. Since all of the condensers in MED operate at subatmospheric levels, it is a suitable approximation to ignore pressure effects on the condensing side.

4. Parametric comparison of MED models

A parametric study is conducted in which the present model is compared to four models from the literature [5–8]. Performance ratio and specific area are evaluated for each of the models while varying the number of effects, steam temperature, or recovery ratio. In order to ensure that the values of the calculated heat transfer area from one model to the next are comparable, heat transfer coefficients in all models were evaluated using Eqs. (11), (24), and (28), rather than assuming the constant values that were given in the respective papers.

All of the calculations in this section are evaluated under the so-called "on-design" analysis method in which temperature differences, flow rates, and other desired operating conditions are inputs and heat transfer areas and other sizing parameters are evaluated as outputs. This is different from "off-design" analysis in which plant sizing information is used to calculate temperature differences, flow rates, and other operating conditions. A consequence of on-design analysis is that each of the data points presented below represent a different physical plant.

For the following parametric studies, all of the following inputs are held constant except for the parameter that is being investigated: number of effects, 8; steam temperature, 70 °C; last effect temperature, 40 °C; seawater temperature, 25 °C; minimum feed heater TTD, 5 K; temperature rise in condenser, 10 K; BPE/thermodynamic losses, 1 K; feed salinity, 42 g/kg; recovery ratio, 0.4; mass flow rate of distillate produced, 1 kg/s.

The Darwish model uses top brine temperature, rather than steam temperature. For convenience, the same value of T_S is used for TBT. The effect of this is that the Darwish models are being evaluated as if a slightly higher steam temperature is being used (approximately 2-5 K, depending on the number of effects). Using the value of T_S in place of TBT introduces some

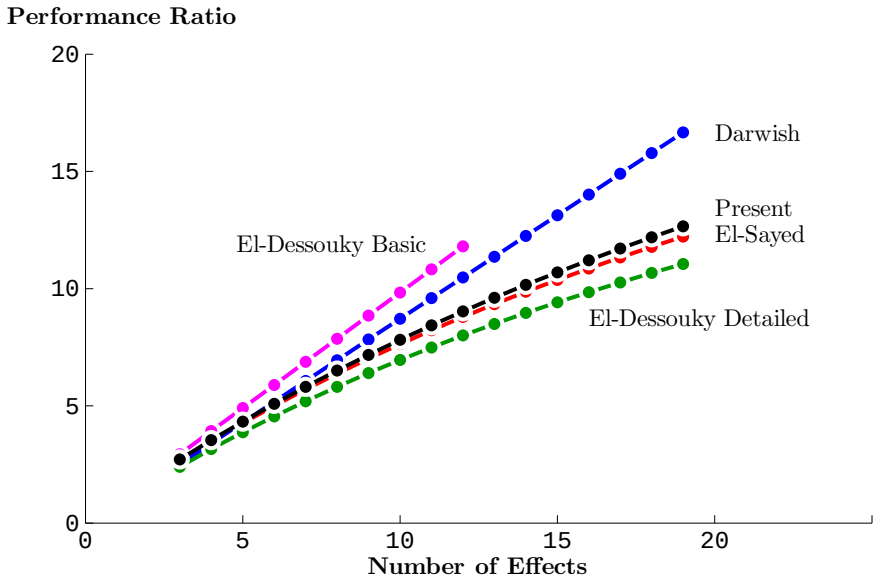

Figure 6: The added benefit of number of effects on the performance ratio should decrease as n increases as seen by the PR behavior of the El-Sayed, El-Dessouky Detailed, and present models. El-Dessouky Basic and Darwish significantly overestimate PR for large number of effects.

minor quantitative differences, but the general trends observed are unchanged. Additionally, the Darwish model does not include calculation of the condenser surface area whereas the other models do.

4.1. Effect of number of effects

The number of effects is generally considered to be one of the strongest determinants of an MED system's performance. Each additional effect allows for an additional evaporation process in which the heat of vaporization is reused an additional time. In the absence of thermodynamic losses, as the vapor condenses, it would release enough heat to exactly evaporate the same amount of new vapor. Therefore, in the ideal case, each additional effect would increase the performance ratio by one. As a result of losses as well as an increasing heat of vaporization with decreasing saturation temperature, it is observed that each additional effect increases the performance ratio by less than one. Further, the added benefit of each additional effect decreases [8]. The present model, El-Sayed's model, and El-Dessouky's detailed model all show this trend of PR increasing with n, with the effect decreasing as n increases (Fig. 6). The basic El-Dessouky model and the Darwish model, however, show PR being a nearly linear function of n. Both of these models over-estimate PR at higher number of effects and fail to capture the effect of increasing latent heat with decreasing saturation temperature. Additionally, El-Dessouky basic assumes that the feed enters the first effect at the effect's saturation temperature which implicitly implies that there is perfect energy regeneration (*i.e.*, $\mathrm{TTD}_{fh} = 0$).

Size of an MED plant is also strongly dependent on the number of effects. During the on-design process, adding additional effects results in a smaller driving temperature difference in each effect and lower distillate production in each effect. Therefore, specific heat transfer area increases with number of effects (Fig. 7). The models by El-Dessouky (Basic), El-Sayed, and Darwish all show SA growing faster with increasing n than does the new model or the detailed El-Dessouky model. All three models assume constant thermodynamic losses (primarily, BPE) in each effect and over-estimate the value of BPE. Equation (10) shows that A_e is inversely proportional to the difference between the previous effect's saturation temperature and the current effect's actual temperature, $T^{\mathrm{prev}}_{D,\mathrm{sat}} - T_e$. Using Eq. (9), this temperature difference can

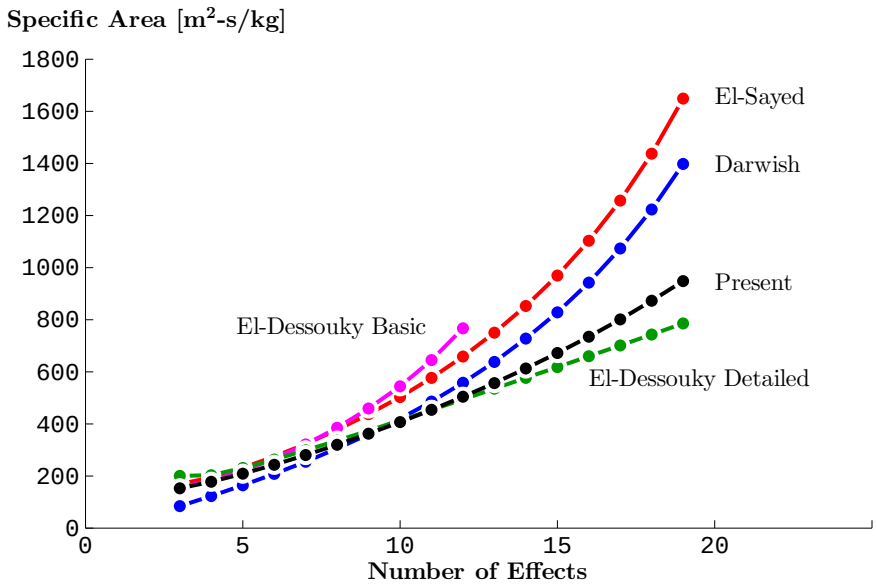

Figure 7: The required surface area increases nearly exponentially with number of effects. As the number of effects increase, the driving temperature difference decreases, thus requiring additional heat transfer area in order to produce the same amount of distillate.

be written as $T_e^{\text{prev}} - T_e - \text{BPE}_D$. Since these models approximate the temperature difference between effects to be constant and equal to $(T_{\max} - T_{\min})/n$, as n increases while temperature range and BPE remain constant, the driving temperature difference in each effect decreases resulting in a dramatic increase in required heat transfer area in each effect. By properly evaluating BPE for each effect as a function of temperature and salinity, A_e can be more accurately calculated. Additionally, modifying the El-Sayed and Darwish models by calculating BPE at each effect using the correlation provided by Sharqawy et al. [28] results in the two models' prediction of SA to agree with the present model within 10% (Fig. 8). The basic model by El-Dessouky predicts the highest specific area since it assumes no flashing in any of the effects. As a result, all distillate is produced through boiling heat transfer. Correcting the model for BPE and approximating that 10% of the distillate is produced by flashing (typical value based on the other models), the El-Dessouky model calculation of SA also agrees with the present model within 10%.

It is observed that the assumptions of constant overall heat transfer coefficient, latent heat of evaporation, and distillate production in each effect have a minimal effect on the evaluation of overall surface area. The Darwish model predicts a lower specific area for small number of effects than the other models since it does not include the area of the condenser. The size of the condenser is largest for a smaller number of effects since the distillate produced in the last effect increases with decreasing n.

4.2. Effect of steam temperature

Increasing top temperature tends to increase the performance of thermodynamic systems. However, in the case of on-design analysis, this is not always the case. The main benefit of increasing the top temperature of an MED system is that it creates a larger temperature range for the desalination process which allows for additional effects. However, when keeping the number of effects fixed and allowing the size of the effects to vary, increasing the top temperature does not have the expected effect on the performance ratio. Since the heat of vaporization decreases with increasing steam temperature, all other things held constant, more steam is needed to evaporate a given quantity of water when the steam is at higher temperature.

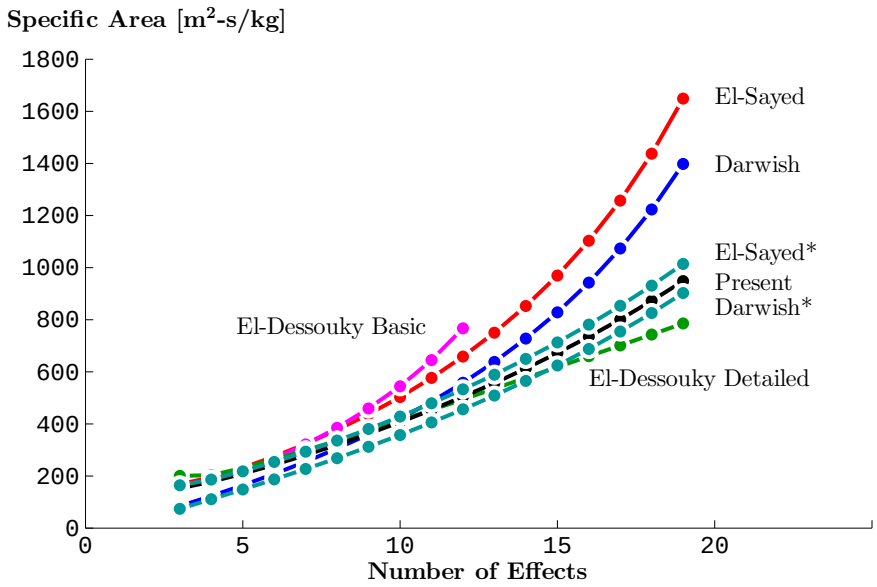

Figure 8: Modifying the Darwish and El-Sayed models by evaluating boiling point elevation as a function of temperature and salinity in each effect causes both models to predict specific area requirements that are in agreement with El-Dessouky's detailed model and the present model. El-Dessouky's basic model can be modified similarly but is not shown for clarity.

As a result, PR decreases slightly with increasing steam temperature. All five models illustrate this behavior (Fig. 9).

While higher temperature steam provides less energy during condensation due to a lessened heat of vaporization, the increased temperature range of the MED system results in a larger temperature difference between each effect. Since the heat transfer within each effect is governed by Newton's Law of Cooling, where the relevant temperature difference is that between the condensing distillate and the evaporating feed, heat transfer increases with increasing ΔT. Since the number of effects and the total distillate flow rate is held constant for this analysis, the amount of heat transfer in each effect remains approximately constant. Therefore, as the driving temperature difference increases, the required heat transfer area decreases. Again, all five models illustrate this trend (Fig. 10).

4.3. Effect of recovery ratio

Increasing the recovery ratio, defined as the amount of distillate produced per input feed, has the effect of reducing the amount of feed seawater since the mass flow rate of distillate produced is held constant. Reducing the amount of feed in the system lowers the thermal mass that must be heated by steam. Therefore, for fixed distillate production, an increased recovery ratio decreases the amount of required steam and the performance ratio increases. The models by both Darwish and El-Sayed as well as the present model all follow this trend (Fig. 11). The El-Dessouky basic model, however, calculates the required steam flow rate based purely on the distillate flow rate, and therefore, is not a function of recovery.

Another consequence of decreasing the feed flow rate is that less feed enters each effect resulting in less distillate vapor produced per effect. Since the amount of total distillate produced needs to remain roughly constant, more distillate must be produced by boiling to make up for the decrease in production from flashing. In order to allow for additional vapor production from boiling, more heat transfer area is required to allow for increased heat transfer. As before, the models by Darwish and El-Sayed, as well as the present model follow this trend while the El-Dessouky basic model is not a function of recovery ratio (Fig. 12).

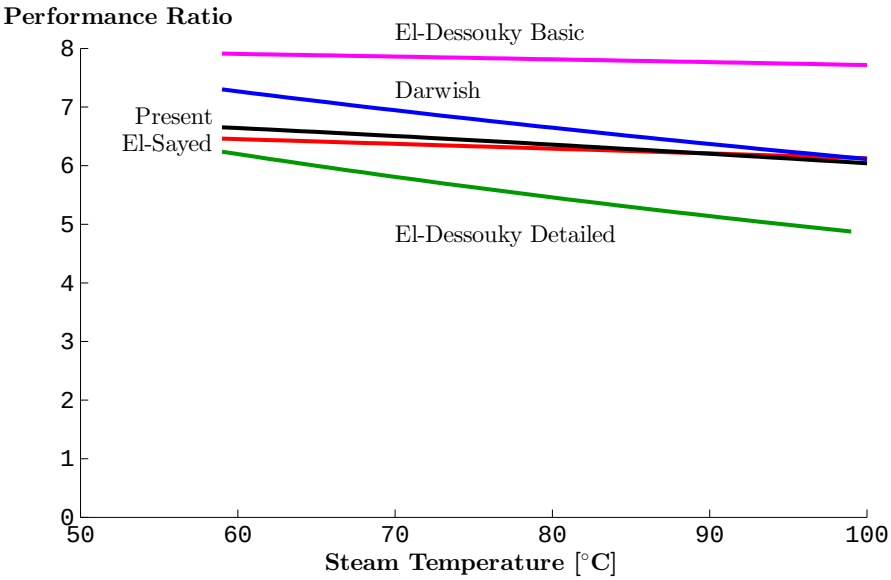

Figure 9: The performance ratio decreases with increasing steam temperature because the heat of vaporization decreases with increasing temperature. The decrease in heat of vaporization results in additional steam needed to evaporate a given unit of water.

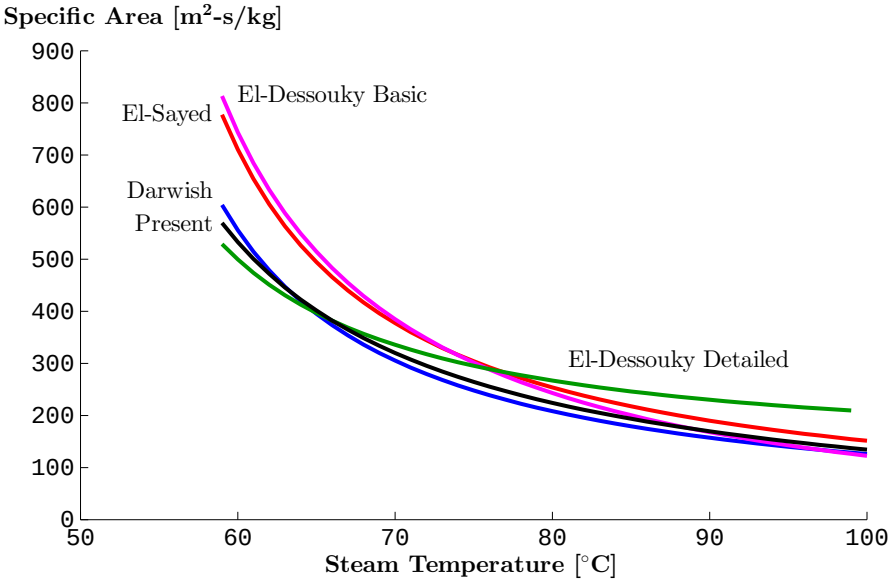

Figure 10: The driving temperature difference between each effect is increased as the steam temperature increases, thus resulting in smaller heat transfer area requirements.

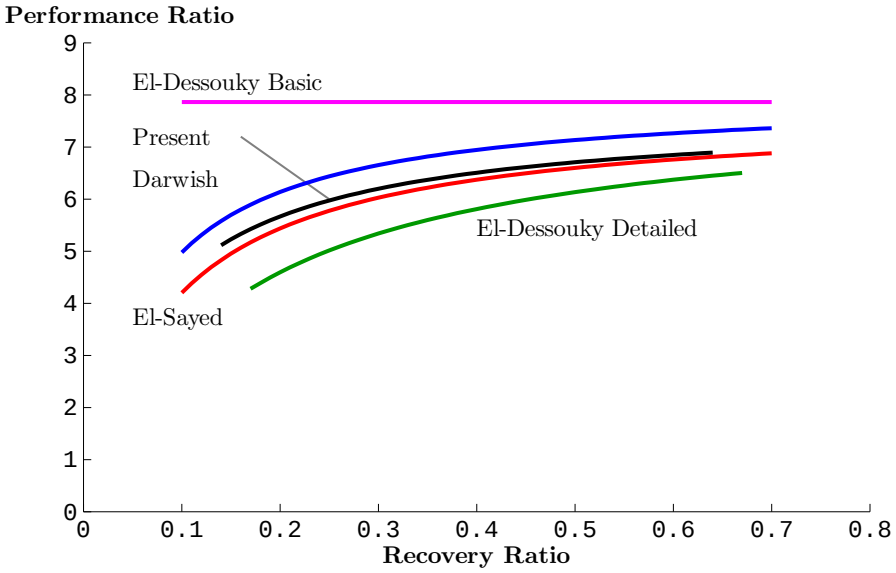

Figure 11: As the recovery ratio increases for fixed distillate production, the feed flow rate reduces resulting in less heating steam required, and therefore, a higher performance ratio.

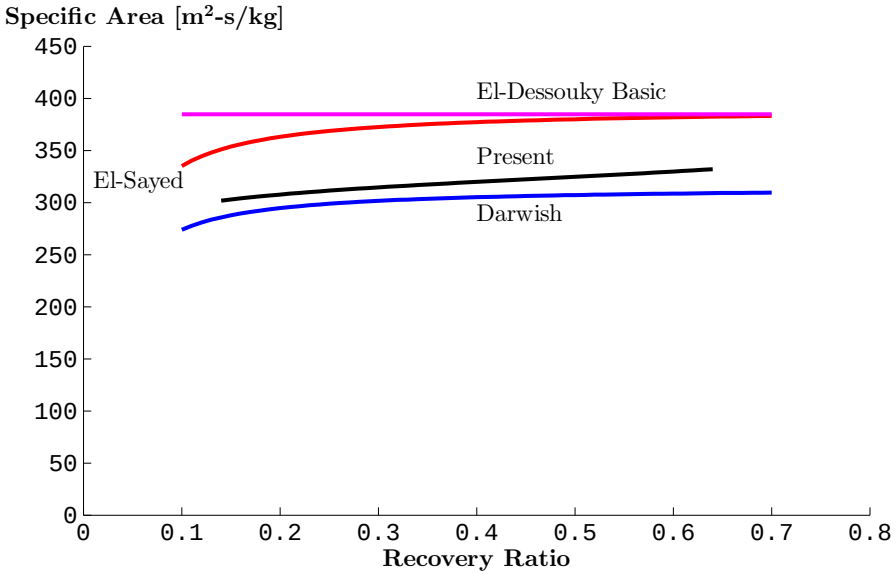

Figure 12: As the recovery ratio increases for fixed distillate production, the feed flow rate reduces resulting in less vapor produced by flashing in each effect. In order to maintain a constant distillate production rate, more distillate must evaporate through boiling, and therefore, more surface area is required.

5. Main findings and key results

Based on a parametric study of the five models, the following conclusions are made:

1. A detailed model is needed in order to properly capture sensitivities of parameters relevant in cogeneration system analysis. The MED model should respond to changes in design conditions (number of effects, terminal temperature differences, *etc.*), input conditions (feed temperature, salinity, flow rate, steam temperature, *etc.*), and operating conditions (recovery ratio, last effect temperature, *etc.*).

2. Use of a simultaneous equation solver allows for the development of more complex numerical models without having to worry about developing solution algorithms. Therefore, fewer major approximations are needed in order to develop an easily solvable model.

3. While the model presented in this paper provides more detail than the existing models from literature while relying on fewer assumptions, several of the existing models provide consistent results. If only basic information about the system is desired for simple studies (*e.g.*, performance ratio and specific heat transfer area), the simpler models may be sufficient. If, however, detailed information about the area of each component and various temperature profiles are required, the present model is preferable.

4. Approximations such as constant thermodynamic losses, constant properties, and constant distillate production in each effect break down with increasing number of effects. Of these approximations, thermodynamic losses (specifically boiling point elevation) have the greatest effect on the evaluation of specific area.

5. A modular model allows for easily studying various MED configurations such as forward feed and parallel feed without developing new code for each of the subcomponents.

6. Acknowledgments

The authors would like to thank the King Fahd University of Petroleum and Minerals in Dhahran, Saudi Arabia, for funding the research reported in this paper through the Center for Clean Water and Clean Energy at MIT and KFUPM under project number R13-CW-10. The authors would also like to thank Numerica Technology for providing access to the JACOBIAN software for this research.

Nomenclature

Roman Symbols

A_c	heat transfer area in condenser	m^2
A_e	heat transfer area in effect	m^2
A_{fh}	heat transfer area in feed heater	m^2
B	brine flow rate from effect	kg/s
B_e	brine flow rate in effect after flashing, before boiling	kg/s
c	specific heat at constant pressure	kJ/kg-K
D	total distillate from effect	kg/s
D_b	distillate from boiling in effect	kg/s
D_c	distillate that will condense in effect	kg/s
D_f	distillate from flashing in effect	kg/s
D_{bd}	distillate blow down from flash box	kg/s
D_{fb}	distillate from flash box	kg/s
F	feed flow rate into effect	kg/s
h	specific enthalpy	kJ/kg
h_{fg}	specific heat of vaporization	kJ/kg
i	i^{th} effect	-
$\dot{m}_{\text{cond}}$	mass flow rate of seawater in condenser	kg/s
$\dot{m}_{sw}$	input seawater flow rate	kg/s
$\dot{m}_B$	final brine flow rate	kg/s
$\dot{m}_D$	distillate flow rate	kg/s
$\dot{m}_F$	feed water flow rate	kg/s
$\dot{m}_S$	input steam flow rate	kg/s
$\dot{m}_{cw}$	cooling water flow rate	kg/s
n	number of effects	-
p	pressure	kPa
ΔT_e	temperature difference between effects	K
T	temperature	K
U_c	overall heat transfer coefficient in condenser	kW/m^2-K

U_e	overall heat transfer coefficient in effect	kW/m^2-K
U_{fh}	overall heat transfer coefficient in feed heater	kW/m^2-K
X	salinity	kg/kg
y	quality	kg/kg

Greek Symbols

ϵ	sum of BPE and temperature change due to pressure loss	K

Subscripts

c	condenser
e	effect
fh	feed heater
sat	saturated, at saturation temperature
sat, f	saturated liquid
sat, g	saturated vapor
sw	seawater
S	steam

Superscripts

in	in flow to CV
out	out flow from CV
prev	previous

Acronyms

BPE	boiling point elevation	K
CV	control volume	
FF	forward feed	
GOR	gained output ratio	-
LMTD	log mean temperature difference	K
MED	multiple effect distillation	
MSF	multistage flash	
NEA	non-equilibrium allowance	K

PR	performance ratio	-
RR	recovery ratio	-
SA	specific area	m^2-s/kg
TBT	top brine temperature	K
TTD	terminal temperature difference	K
TVC	thermal vapor compressor	

References

[1] F. Alasfour, M. Darwish, A. B. Amer, Thermal analysis of ME-TVC+MEE desalination systems, Desalination 174 (2005) 39–61.

[2] A. Ophir, F. Lokiec, Advanced med process for most economical sea water desalination, Desalination 182 (2005) 187–198. Desalination and the Environment.

[3] M. Darwish, A. Alsairafi, Technical comparison between tvc/meb and msf, Desalination 170 (2004) 223–239.

[4] K. H. Mistry, R. K. McGovern, G. P. Thiel, E. K. Summers, S. M. Zubair, J. H. Lienhard V, Entropy generation analysis of desalination technologies, Entropy 13 (2011) 1829–1864.

[5] H. El-Dessouky, I. Alatiqi, S. Bingulac, H. Ettouney, Steady-State Analysis of the Multiple Effect Evaporation Desalination Process, Chemical Engineering & Technology 21 (1998) 437–451.

[6] H. T. El-Dessouky, H. M. Ettouney, Fundamentals of Salt Water Desalination, Elsevier, Amsterdamn, The Netherlands, 2002.

[7] M. Darwish, F. Al-Juwayhel, H. K. Abdulraheim, Multi-effect boiling systems from an energy viewpoint, Desalination 194 (2006) 22–39.

[8] Y. M. El-Sayed, R. S. Silver, Principles of Desalination, volume A, Academic Press, New York, NY, 2nd edition, pp. 55–109.

[9] H. T. El-Dessouky, H. Ettouney, Multiple-effect evaporation desalination systems. thermal analysis, Desalination 125 (1999) 259–276. European Conference on Desalination and the Environment.

[10] H. T. El-Dessouky, H. M. Ettouney, F. Mandani, Performance of parallel feed multiple effect evaporation system for seawater desalination, Applied Thermal Engineering 20 (2000) 1679–1706.

[11] M. Darwish, H. K. Abdulrahim, Feed water arrangements in a multi-effect desalting system, Desalination 228 (2008) 30–54.

[12] M. El-Allawy, Predictive simulation of the performance of med/tvc desalination distiller, in: IDA Conference, International Desalination Association, Bahams.

[13] N. H. Aly, A. K. El-Figi, Thermal performance of seawater desalination systems, Desalination 158 (2003) 127–142. Desalination and the Environment: Fresh Water for All.

[14] M. Al-Sahali, H. Ettouney, Developments in thermal desalination processes: Design, energy, and costing aspects, Desalination 214 (2007) 227–240.

[15] M. Ameri, S. S. Mohammadi, M. Hosseini, M. Seifi, Effect of design parameters on multi-effect desalinationsystem specifications, Desalination 245 (2009) 266–283. Engineering with Membranes 2008 - Membrane Processes: Development, Monitoring and Modelling From the Nano to the Macro Scale, Engineering with Membranes 2008.

[16] R. Kamali, S. Mohebinia, Experience of design and optimization of multi-effects desalination systems in iran, Desalination 222 (2008) 639–645. European Desalination Society and Center for Research and Technology Hellas (CERTH), Sani Resort 22-25 April 2007, Halkidiki, Greece European Desalination Society and Center for Research and Technology Hellas (CERTH), Sani Resort.

[17] R. Kamali, A. Abbassi, S. S. Vanini, M. S. Avval, Thermodynamic design and parametric study of med-tvc, Desalination 222 (2008) 596–604. European Desalination Society and Center for Research and Technology Hellas (CERTH), Sani Resort 22 -25 April 2007, Halkidiki, Greece, European Desalination Society and Center for Research and Technology Hellas (CERTH), Sani Resort.

[18] K. Minnich, J. Tonner, D. Neu, A comparison for heat transfer requirement and evaporator cost for med/tvc and msf, in: IDA Conference, International Desalination Association, Abu Dhabi, UAE.

[19] H.-S. Choi, T.-J. Lee, Y.-G. Kim, S.-L. Song, Performance improvement of multiple-effect distiller with thermal vapor compression system by exergy analysis, Desalination 182 (2005) 239–249. Desalination and the Environment Desalination and the Environment.

[20] M. Darwish, N. Al-Najem, Energy consumptions and costs of different desalting systems, Desalination 64 (1987) 83–96.

[21] N. M. Al-Najem, M. Darwish, F. Youssef, Thermovapor compression desalters: energy and availability — analysis of single- and multi-effect systems, Desalination 110 (1997) 223–238.

[22] O. Hamed, Thermal assessment of a multiple effect boiling (meb) desalination system, Desalination 86 (1992) 325–339.

[23] O. Hamed, A. Zamamiri, S. Aly, N. Lior, Thermal performance and exergy analysis of a thermal vapor compression desalination system, Energy Conversion and Management 37 (1996) 379–387.

[24] A. Greogorzewski, K. Genthner, Multieffect distillation: A study and comparison of different process configuration, in: IDA Conference, International Desalination Association, Abu Dhabi, UAE.

[25] The MathWorks, MATLAB R2011a, Software, 2011.

[26] S. A. Klein, Engineering Equation Solver, Academic Professional, Version 8, Software, 2010.

[27] Numerica Technology, JACOBIAN Modeling and Optimization Software, `http://www.numericatech.com`, 2009. Accessed March 2010.

[28] M. H. Sharqawy, J. H. Lienhard V, S. M. Zubair, Thermophysical properties of seawater: A review of existing correlations and data, Desalination and Water Treatment 16 (2010) 354–380.

[29] W. Wagner, A. Pruss, The IAPWS Formulation 1995 for the Thermodynamic Properties of Ordinary Water Substance for General and Scientific Use, Journal of Physical and Chemical Reference Data 31 (2002) 387–535.

[30] J. R. Cooper, Revised Release on the IAPWS Industrial Formulation 1997 for the Thermodynamic Properties of Water and Steam, The International Association for the Properties of Water and Steam (2007) 1–48.

[31] A. C. Mueller, Heat Exchanger Design Handbook, volume 3: Thermal and hydraulic design of heat exchangers, Hemisphere Publishing Corporation, Washington, pp. 3.4.7–1–3.4.7–2.